Singular Integral Equation Method for Interaction Between Elliptical Inclusions

Nao-Aki Noda
Department of Mechanical Engineering,
Kyushu Institute of Technology,
Kitakyushu 804-8550, Japan

Tadatoshi Matsuo
Department of Mechanical Engineering,
Fukushima National College of Technology,
Iwaki 970-8034, Japan

This paper deals with numerical solutions of singular integral equations in interaction problems of elliptical inclusions under general loading conditions. The stress and displacement fields due to a point force in infinite plates are used as fundamental solutions. Then, the problems are formulated as a system of singular integral equations with Cauchy-type or logarithmic-type singularities, where the unknowns are the body force densities distributed in infinite plates having the same elastic constants as those of the matrix and inclusions. To determine the unknown body force densities to satisfy the boundary conditions, four auxiliary unknown functions are derived from each body force density. It is found that determining these four auxiliary functions in the range $0 \leqq \phi_k \leqq \pi/2$ is equivalent to determining an original unknown density in the range $0 \leqq \phi_k \leqq 2\pi$. Then, these auxiliary unknowns are approximated by using fundamental densities and polynomials. Initially, the convergence of the results such as unknown densities and interface stresses are confirmed with increasing collocation points. Also, the accuracy is verified by examining the boundary conditions and relations between interface stresses and displacements. Randomly or regularly distributed elliptical inclusions can be treated by combining both solutions for remote tension and shear shown in this study.

1 Introduction

Elliptical inclusions can be regarded as a general model of defects because they cover a wide variety of particular cases, such as line and circular defects. The stress concentration due to two or more defects differs from that due to an isolated defect. Interaction among cracks can be treated using singular integral equations using the related Green's function for an edge dislocation (Erdogan et al., 1972). In this paper, the general solution for elliptical inclusions will be discussed. To formulate the problem, the body-force method is applied.

In the conventional body-force method, the unknown functions of the body-force densities have been approximated by the products of the fundamental density functions and weight functions. Here,

(a) the fundamental density function is an exact density of body force to express a two-dimensional single elliptical hole, and
(b) the weight function is chosen to be a "step function," which takes a constant value along each segment into which a whole boundary is discretized (Nisitani, 1963, 1967).

In previous papers, numerical solutions of the singular integral equation of the body-force method for elliptical holes was discussed (Noda-Matsuo, 1995a, b, 1997). Then it was found that in the conventional method, unknown body-force densities distributed in two directions in plates do not converge with increasing collocation points. The reason was indicated that conventional two-type body-force densities cannot represent the actual density distributions enough especially near the apex of elliptical boundaries. To overcome this difficulty, eight fundamental densities were newly introduced, and the body-force densities were approximated by a linear combination of fundamental densities and polynomials.

The objects of this paper are follows:

1 to show the solution of elliptical inclusions that can be regarded as a general model of defects. The method is essentially based on the solution proposed for solving elliptical holes. However, the applicability of several fundamental densities proposed previously to inclusion problems is not obvious and therefore it should be confirmed in this study.

2 to explain the meaning of the new fundamental densities proposed by the authors more clearly. It has been told that the discussion of the theory shown in previous papers is of little pedagogical value because it cryptically presents the governing equations with no derivation. In this paper, therefore, auxiliary functions will be derived from original unknown densities of the singular integral equations. Then it will be shown that new fundamental densities are useful for approximating these auxiliary functions. Finally, original unknown densities will be expressed from obtained auxiliary functions.

2 Singular Integral Equations of the Body Force Method for Inclusion Problems

Consider an infinite plate with two elliptical inclusions ($x = \pm d + a\cos\theta$, $y = b\sin\theta$) under remote tension or shear as shown in Figs. 1 or 2 to explain the numerical solution. This method may be applied to regular or random distribution of inclusions. The problem can be formulated in terms of singular integral equations by using the stress and displacement fields due to a point force in two infinite plates "M" and "I". Here, the infinite plate "M" has the same elastic constants as those of the matrix (E_M, ν_M) and the infinite plate "I" has the same ones as those of the inclusions (E_I, ν_I). The integral equations are expressed in Eqs. (1) and (2), where the body-force densities distributed in the infinite plates M and I in the x, y-directions are unknown functions (see Fig. 3).

Contributed by the Applied Mechanics Division of THE AMERICAN SOCIETY OF MECHANICAL ENGINEERS for publication in the ASME JOURNAL OF APPLIED MECHANICS.

Discussion on the paper should be addressed to the Technical Editor, Professor Lewis T. Wheeler, Department of Mechanical Engineering, University of Houston, Houston, TX 77204-4792, and will be accepted until four months after final publication of the paper itself in the ASME JOURNAL OF APPLIED MECHANICS.

Manuscript received by the ASME Applied Mechanics Division, Feb. 13, 1995; final revision, Mar. 2, 1998. Associate Technical Editor: X. Markenscoff.

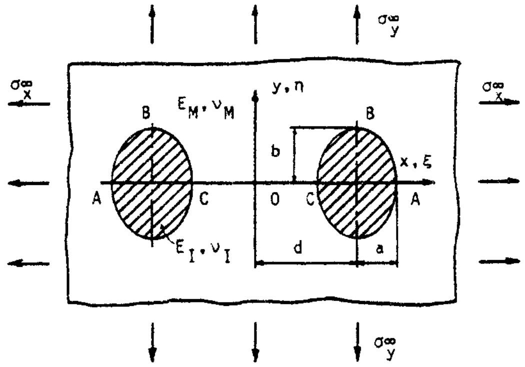

Fig. 1 Two elliptical inclusions in an infinite plate under remote tension

$$-(1/2)\{\rho^*_{xM}(\theta_i)\cos\theta_{i0}+\rho^*_{yM}(\theta_i)\sin\theta_{i0}\}$$
$$-(1/2)\{\rho^*_{xI}(\theta_i)\cos\theta_{i0}+\rho^*_{yI}(\theta_i)\sin\theta_{i0}\}$$
$$+\sum_{k=1}^{2}\int_0^{2\pi}K^{Fx}_{nnM}(\phi_k,\theta_i)\rho^*_{xM}(\phi_k)ds$$
$$+\sum_{k=1}^{2}\int_0^{2\pi}K^{Fy}_{nnM}(\phi_k,\theta_i)\rho^*_{yM}(\phi_k)ds$$
$$-\sum_{k=1}^{2}\int_0^{2\pi}K^{Fx}_{nnI}(\phi_k,\theta_i)\rho^*_{xI}(\phi_k)ds$$
$$-\sum_{k=1}^{2}\int_0^{2\pi}K^{Fy}_{nnI}(\phi_k,\theta_i)\rho^*_{yI}(\phi_k)ds=-\sigma^\infty_n$$

$$-(1/2)\{-\rho^*_{xM}(\theta_i)\sin\theta_{i0}+\rho^*_{yM}(\theta_i)\cos\theta_{i0}\}$$
$$-(1/2)\{-\rho^*_{xI}(\theta_i)\sin\theta_{i0}+\rho^*_{yI}(\theta_i)\cos\theta_{i0}\}$$
$$+\sum_{k=1}^{2}\int_0^{2\pi}K^{Fx}_{ntM}(\phi_k,\theta_i)\rho^*_{xM}(\phi_k)ds$$
$$+\sum_{k=1}^{2}\int_0^{2\pi}K^{Fy}_{ntM}(\phi_k,\theta_i)\rho^*_{yM}(\phi_k)ds$$
$$-\sum_{k=1}^{2}\int_0^{2\pi}K^{Fx}_{ntI}(\phi_k,\theta_i)\rho^*_{xI}(\phi_k)ds$$
$$-\sum_{k=1}^{2}\int_0^{2\pi}K^{Fy}_{ntI}(\phi_k,\theta_i)\rho^*_{yI}(\phi_k)ds=-\tau^\infty_{nt}\quad i=1,2 \qquad (1)$$

$$\sum_{k=1}^{2}\int_0^{2\pi}K^{Fx}_{uM}(\phi_k,\theta_i)\rho^*_{xM}(\phi_k)ds$$
$$+\sum_{k=1}^{2}\int_0^{2\pi}K^{Fy}_{uM}(\phi_k,\theta_i)\rho^*_{yM}(\phi_k)ds$$
$$-\sum_{k=1}^{2}\int_0^{2\pi}K^{Fx}_{uI}(\phi_k,\theta_i)\rho^*_{xI}(\phi_k)ds$$
$$-\sum_{k=1}^{2}\int_0^{2\pi}K^{Fy}_{uI}(\phi_k,\theta_i)\rho^*_{yI}(\phi_k)ds=-U^\infty$$

$$\sum_{k=1}^{2}\int_0^{2\pi}K^{Fx}_{vM}(\phi_k,\theta_i)\rho^*_{xM}(\phi_k)ds$$
$$+\sum_{k=1}^{2}\int_0^{2\pi}K^{Fy}_{vM}(\phi_k,\theta_i)\rho^*_{yM}(\phi_k)ds$$
$$-\sum_{k=1}^{2}\int_0^{2\pi}K^{Fx}_{vI}(\phi_k,\theta_i)\rho^*_{xI}(\phi_k)ds$$
$$-\sum_{k=1}^{2}\int_0^{2\pi}K^{Fy}_{vI}(\phi_k,\theta_i)\rho^*_{yI}(\phi_k)ds=-V^\infty\quad i=1,2 \qquad (2)$$

where

$$\sigma^\infty_n=\sigma^\infty_x\cos^2\theta_{i0}+\sigma^\infty_y\sin^2\theta_{i0},$$
$$\tau^\infty_{nt}=(\sigma^\infty_y-\sigma^\infty_x)\sin\theta_{i0}\cos\theta_{i0},$$
$$U^\infty=(\sigma^\infty_x-\nu_M\sigma^\infty_y)x/E_M,$$
$$V^\infty=(\sigma^\infty_y-\nu_M\sigma^\infty_x)y/E_M\quad\text{(for Fig. 1)};$$
$$\sigma^\infty_n=2\tau^\infty_{xy}\sin\theta_{i0}\cos\theta_{i0},\quad \tau^\infty_{nt}=\tau^\infty_{xy}(\cos^2\theta_{i0}-\sin^2\theta_{i0}),$$
$$U^\infty=2(1+\nu_M)\tau^\infty_{xy}y/E_M,$$
$$V^\infty=2(1+\nu_M)\tau^\infty_{xy}x/E_M\quad\text{(for Fig. 2)};$$
$$-d\xi=a\sin\phi_k d\phi,\quad d\eta=b\cos\phi_k d\phi,$$
$$ds=\sqrt{a^2\sin^2\phi_k+b^2\cos^2\phi_k}\,d\phi,$$
$$\tan\theta_{i0}=(a/b)\tan\theta_i \qquad (3)$$

Here, θ_{i0} is the angle between x-axis and the normal direction at the point (x, y) on the elliptical hole.

The body-force densities $\rho^*_{xM}(\phi_k)$, $\rho^*_{yM}(\phi_k)$, $\rho^*_{xI}(\phi_k)$, $\rho^*_{yI}(\phi_k)$ are defined as follows:

$$\rho^*_{xM}(\phi_k)=\frac{dF_\xi}{ds},\quad \rho^*_{yM}(\phi_k)=\frac{dF_\eta}{ds},$$
$$\rho^*_{xI}(\phi_k)=\frac{dF_\xi}{ds},\quad \rho^*_{yI}(\phi_k)=\frac{dF_\eta}{ds}, \qquad (4)$$

where dF_ξ, dF_η are the components of the resultant of the body force in the x and y-directions acting on the infinitesimal arc length ds, respectively.

Suppose that σ_{nM}, τ_{ntM}, U_M, V_M denote the stress and displacement along the imaginary boundary of elliptical hole in the infinite plate "M." In addition, σ_{nI}, τ_{ntI}, U_I, V_I denote the stress and displacement along the imaginary boundary of elliptical inclusions in the infinite plate "I." Equations (1), (2) enforce the boundary conditions at the connecting boundary of matrix and inclusion; that is, $\sigma_{nM}-\sigma_{nI}=0$, $\tau_{ntM}-\tau_{ntI}=0$, $U_M-U_I=0$, $V_M-V_I=0$. The first and second terms of Eqs. (1) represent the stress due to the body force distributed on "minus boundary". Here "minus boundaries" means the imaginary boundary composed of the internal points that are infinitesimally apart from the initial boundary (Nisitani, 1967). Taking

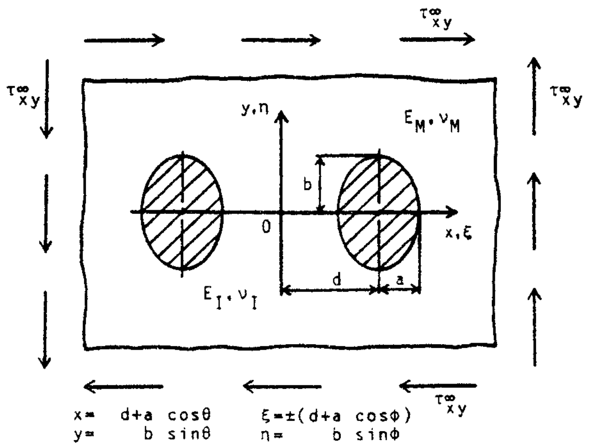

Fig. 2 Two elliptical inclusions in an infinite plate under remote shear

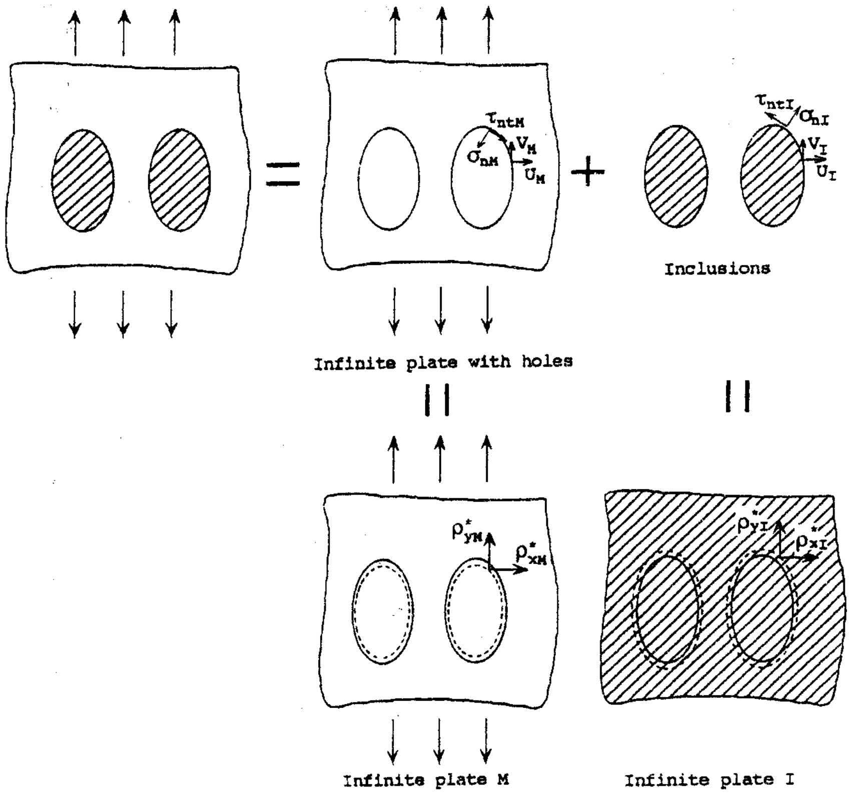

Fig. 3 Formulation of the singular integral equation based on the body-force method

$K^{Fx}_{nnM}(\phi_k, \theta_i)$ for example, the notation means the normal stress σ_n induced at the point when the body force with unit density in the x-direction is acting at the infinitesimal arc length on the kth elliptical hole in the infinite plate "M." In the calculation of displacement $K^{Fx}_{uM}(\phi_k, \theta_i)$, etc., the relative displacement with respect to a certain point outside inclusion is considered (Nisitani-Chen, 1987). Equations (1) and (2) include the Cauchy-type and logarithmic-type singularities, respectively, when $i = k$. Therefore, when $\theta = \phi$ and $k = i$, the integration in Eq. (1) should be interpreted as the meaning of Cauchy's principle values.

3 How to Determine Unknown Body Force Densities

3.1 Definition of Auxiliary Functions. To solve Eqs. (1), (2) is to determine the body-force densities $\rho^*_{xM}(\phi_k)$, $\rho^*_{yM}(\phi_k)$, $\rho^*_{xI}(\phi_k)$, $\rho^*_{yI}(\phi_k)$ in the range $0 \leqq \phi_k \leqq 2\pi$. Here, by taking examples $\rho^*_{xM}(\phi_k)$, $\rho^*_{yM}(\phi_k)$ how to determine unknown functions will be explained. Consider auxiliary functions $\rho^*_{xM1}(\phi_k) \sim \rho^*_{xM4}(\phi_k)$, and $\rho^*_{yM1}(\phi_k) \sim \rho^*_{yM4}(\phi_k)$ defined by Eqs. (5), (6) instead of $\rho^*_{xM}(\phi_k)$, $\rho^*_{yM}(\phi_k)$.

$$\rho^*_{xM1}(\phi_k) = \{\rho^*_{xM}(\phi_k) + \rho^*_{xM}(\pi - \phi_k) + \rho^*_{xM}(\pi + \phi_k) + \rho^*_{xM}(-\phi_k)\}/4 \quad (5a)$$

$$\rho^*_{xM2}(\phi_k) = \{\rho^*_{xM}(\phi_k) + \rho^*_{xM}(\pi - \phi_k) - \rho^*_{xM}(\pi + \phi_k) - \rho^*_{xM}(-\phi_k)\}/4 \quad (5b)$$

$$\rho^*_{xM3}(\phi_k) = \{\rho^*_{xM}(\phi_k) - \rho^*_{xM}(\pi - \phi_k) - \rho^*_{xM}(\pi + \phi_k) + \rho^*_{xM}(-\phi_k)\}/4 \quad (5c)$$

$$\rho^*_{xM4}(\phi_k) = \{\rho^*_{xM}(\phi_k) - \rho^*_{xM}(\pi - \phi_k) + \rho^*_{xM}(\pi + \phi_k) - \rho^*_{xM}(-\phi_k)\}/4 \quad (5d)$$

$$\rho^*_{yM1}(\phi_k) = \{\rho^*_{yM}(\phi_k) + \rho^*_{yM}(\pi - \phi_k) + \rho^*_{yM}(\pi + \phi_k) + \rho^*_{yM}(-\phi_k)\}/4 \quad (6a)$$

$$\rho^*_{yM2}(\phi_k) = \{\rho^*_{yM}(\phi_k) + \rho^*_{yM}(\pi - \phi_k) - \rho^*_{yM}(\pi + \phi_k) - \rho^*_{yM}(-\phi_k)\}/4 \quad (6b)$$

$$\rho^*_{yM3}(\phi_k) = \{\rho^*_{yM}(\phi_k) - \rho^*_{yM}(\pi - \phi_k) - \rho^*_{yM}(\pi + \phi_k) + \rho^*_{yM}(-\phi_k)\}/4 \quad (6c)$$

$$\rho^*_{yM4}(\phi_k) = \{\rho^*_{yM}(\phi_k) - \rho^*_{yM}(\pi - \phi_k) + \rho^*_{yM}(\pi + \phi_k) - \rho^*_{yM}(-\phi_k)\}/4 \quad (6d)$$

These new functions $\rho^*_{xM1}(\phi_k) \sim \rho^*_{xM4}(\phi_k)$ and $\rho^*_{yM1}(\phi_k) \sim \rho^*_{yM4}(\phi_k)$ must satisfy Eqs. (7), (8) because of the definition (5), (6).

$$\rho^*_{xM1}(\phi_k) = \rho^*_{xM1}(\pi - \phi_k) = \rho^*_{xM1}(\pi + \phi_k) = \rho^*_{xM1}(-\phi_k) \quad (7a)$$

$$\rho^*_{xM2}(\phi_k) = \rho^*_{xM2}(\pi - \phi_k) = -\rho^*_{xM2}(\pi + \phi_k) = -\rho^*_{xM2}(-\phi_k) \quad (7b)$$

$$\rho^*_{xM3}(\phi_k) = -\rho^*_{xM3}(\pi - \phi_k) = -\rho^*_{xM3}(\pi + \phi_k) = \rho^*_{xM3}(-\phi_k) \quad (7c)$$

$$\rho^*_{xM4}(\phi_k) = -\rho^*_{xM4}(\pi - \phi_k) = \rho^*_{xM4}(\pi + \phi_k) = -\rho^*_{xM4}(-\phi_k) \quad (7d)$$

$$\rho^*_{yM1}(\phi_k) = \rho^*_{yM1}(\pi - \phi_k) = \rho^*_{yM1}(\pi + \phi_k) = \rho^*_{yM1}(-\phi_k) \quad (8a)$$

$$\rho^*_{yM2}(\phi_k) = \rho^*_{yM2}(\pi - \phi_k) = -\rho^*_{yM2}(\pi + \phi_k) = -\rho^*_{yM2}(-\phi_k) \quad (8b)$$

$$\rho^*_{yM3}(\phi_k) = -\rho^*_{yM3}(\pi - \phi_k) = -\rho^*_{yM3}(\pi + \phi_k) = \rho^*_{yM3}(-\phi_k) \quad (8c)$$

$$\rho^*_{yM4}(\phi_k) = -\rho^*_{yM4}(\pi - \phi_k) = \rho^*_{yM4}(\pi + \phi_k) = -\rho^*_{yM4}(-\phi_k) \quad (8d)$$

It should be noted that determining four auxiliary functions $\rho^*_{xM1}(\phi_k) \sim \rho^*_{xM4}(\phi_k)$ and $\rho^*_{yM1}(\phi_k) \sim \rho^*_{yM4}(\phi_k)$ in the range $0 \leqq$

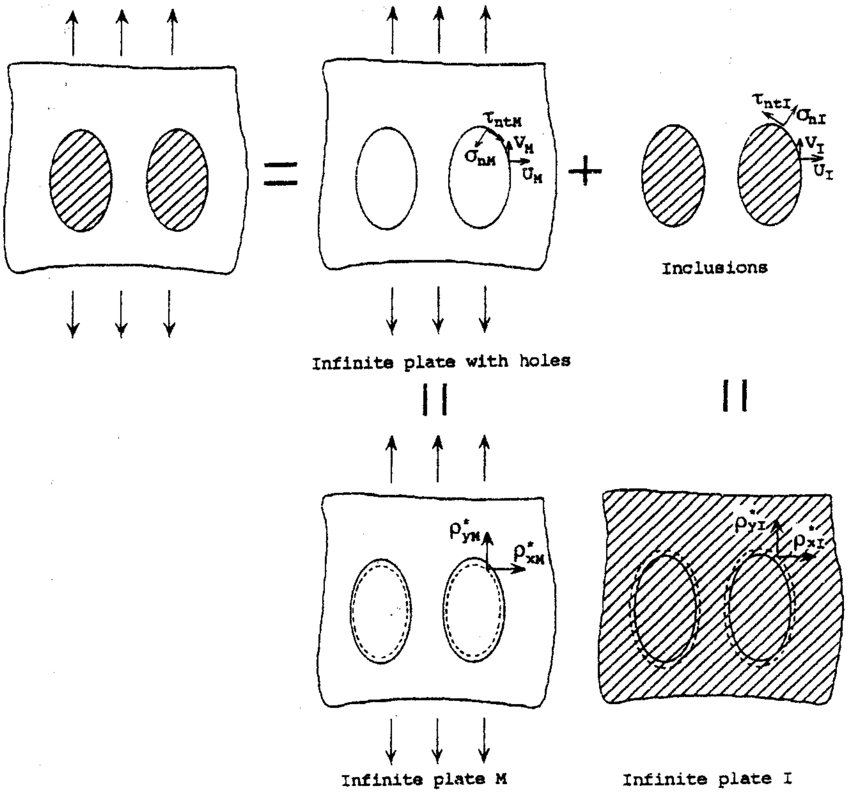

Fig. 3 Formulation of the singular integral equation based on the body-force method

$K^{Fx}_{nnM}(\phi_k, \theta_i)$ for example, the notation means the normal stress σ_n induced at the point when the body force with unit density in the x-direction is acting at the infinitesimal arc length on the kth elliptical hole in the infinite plate "M." In the calculation of displacement $K^{Fx}_{uM}(\phi_k, \theta_i)$, etc., the relative displacement with respect to a certain point outside inclusion is considered (Nisitani-Chen, 1987). Equations (1) and (2) include the Cauchy-type and logarithmic-type singularities, respectively, when $i = k$. Therefore, when $\theta = \phi$ and $k = i$, the integration in Eq. (1) should be interpreted as the meaning of Cauchy's principle values.

3 How to Determine Unknown Body Force Densities

3.1 Definition of Auxiliary Functions. To solve Eqs. (1), (2) is to determine the body-force densities $\rho^*_{xM}(\phi_k)$, $\rho^*_{yM}(\phi_k)$, $\rho^*_{xI}(\phi_k)$, $\rho^*_{yI}(\phi_k)$ in the range $0 \leqq \phi_k \leqq 2\pi$. Here, by taking examples $\rho^*_{xM}(\phi_k)$, $\rho^*_{yM}(\phi_k)$ how to determine unknown functions will be explained. Consider auxiliary functions $\rho^*_{xM1}(\phi_k) \sim \rho^*_{xM4}(\phi_k)$, and $\rho^*_{yM1}(\phi_k) \sim \rho^*_{yM4}(\phi_k)$ defined by Eqs. (5), (6) instead of $\rho^*_{xM}(\phi_k)$, $\rho^*_{yM}(\phi_k)$.

$$\rho^*_{xM1}(\phi_k) = \{\rho^*_{xM}(\phi_k) + \rho^*_{xM}(\pi - \phi_k) + \rho^*_{xM}(\pi + \phi_k) + \rho^*_{xM}(-\phi_k)\}/4 \quad (5a)$$

$$\rho^*_{xM2}(\phi_k) = \{\rho^*_{xM}(\phi_k) + \rho^*_{xM}(\pi - \phi_k) - \rho^*_{xM}(\pi + \phi_k) - \rho^*_{xM}(-\phi_k)\}/4 \quad (5b)$$

$$\rho^*_{xM3}(\phi_k) = \{\rho^*_{xM}(\phi_k) - \rho^*_{xM}(\pi - \phi_k) - \rho^*_{xM}(\pi + \phi_k) + \rho^*_{xM}(-\phi_k)\}/4 \quad (5c)$$

$$\rho^*_{xM4}(\phi_k) = \{\rho^*_{xM}(\phi_k) - \rho^*_{xM}(\pi - \phi_k) + \rho^*_{xM}(\pi + \phi_k) - \rho^*_{xM}(-\phi_k)\}/4 \quad (5d)$$

$$\rho^*_{yM1}(\phi_k) = \{\rho^*_{yM}(\phi_k) + \rho^*_{yM}(\pi - \phi_k) + \rho^*_{yM}(\pi + \phi_k) + \rho^*_{yM}(-\phi_k)\}/4 \quad (6a)$$

$$\rho^*_{yM2}(\phi_k) = \{\rho^*_{yM}(\phi_k) + \rho^*_{yM}(\pi - \phi_k) - \rho^*_{yM}(\pi + \phi_k) - \rho^*_{yM}(-\phi_k)\}/4 \quad (6b)$$

$$\rho^*_{yM3}(\phi_k) = \{\rho^*_{yM}(\phi_k) - \rho^*_{yM}(\pi - \phi_k) - \rho^*_{yM}(\pi + \phi_k) + \rho^*_{yM}(-\phi_k)\}/4 \quad (6c)$$

$$\rho^*_{yM4}(\phi_k) = \{\rho^*_{yM}(\phi_k) - \rho^*_{yM}(\pi - \phi_k) + \rho^*_{yM}(\pi + \phi_k) - \rho^*_{yM}(-\phi_k)\}/4 \quad (6d)$$

These new functions $\rho^*_{xM1}(\phi_k) \sim \rho^*_{xM4}(\phi_k)$ and $\rho^*_{yM1}(\phi_k) \sim \rho^*_{yM4}(\phi_k)$ must satisfy Eqs. (7), (8) because of the definition (5), (6).

$$\rho^*_{xM1}(\phi_k) = \rho^*_{xM1}(\pi - \phi_k) = \rho^*_{xM1}(\pi + \phi_k) = \rho^*_{xM1}(-\phi_k) \quad (7a)$$

$$\rho^*_{xM2}(\phi_k) = \rho^*_{xM2}(\pi - \phi_k) = -\rho^*_{xM2}(\pi + \phi_k) = -\rho^*_{xM2}(-\phi_k) \quad (7b)$$

$$\rho^*_{xM3}(\phi_k) = -\rho^*_{xM3}(\pi - \phi_k) = -\rho^*_{xM3}(\pi + \phi_k) = \rho^*_{xM3}(-\phi_k) \quad (7c)$$

$$\rho^*_{xM4}(\phi_k) = -\rho^*_{xM4}(\pi - \phi_k) = \rho^*_{xM4}(\pi + \phi_k) = -\rho^*_{xM4}(-\phi_k) \quad (7d)$$

$$\rho^*_{yM1}(\phi_k) = \rho^*_{yM1}(\pi - \phi_k) = \rho^*_{yM1}(\pi + \phi_k) = \rho^*_{yM1}(-\phi_k) \quad (8a)$$

$$\rho^*_{yM2}(\phi_k) = \rho^*_{yM2}(\pi - \phi_k) = -\rho^*_{yM2}(\pi + \phi_k) = -\rho^*_{yM2}(-\phi_k) \quad (8b)$$

$$\rho^*_{yM3}(\phi_k) = -\rho^*_{yM3}(\pi - \phi_k) = -\rho^*_{yM3}(\pi + \phi_k) = \rho^*_{yM3}(-\phi_k) \quad (8c)$$

$$\rho^*_{yM4}(\phi_k) = -\rho^*_{yM4}(\pi - \phi_k) = \rho^*_{yM4}(\pi + \phi_k) = -\rho^*_{yM4}(-\phi_k) \quad (8d)$$

It should be noted that determining four auxiliary functions $\rho^*_{xM1}(\phi_k) \sim \rho^*_{xM4}(\phi_k)$ and $\rho^*_{yM1}(\phi_k) \sim \rho^*_{yM4}(\phi_k)$ in the range $0 \leqq$

where M is the number of the collocation points in $0 \leqq \phi \leqq 2\pi$.

Using the approximation method mentioned above, we obtain the following system of linear equations for determining the coefficients a_{nM}, b_{nM}, c_{nM}, d_{nM}, a_{nI}, b_{nI}, c_{nI}, d_{nI}.

$$\sum_{n=1}^{M/2} (a_{nM}A_{nM} + b_{nM}B_{nM} + c_{nM}C_{nM} + d_{nM}D_{nM} + a_{nI}A_{nI} + b_{nI}B_{nI} + c_{nI}C_{nI} + d_{nI}D_{nI}) = -(\sigma_x^\infty \cos^2\theta_{i0} + \sigma_y^\infty \sin^2\theta_{i0})$$

$$\sum_{n=1}^{M/2} (a_{nM}E_{nM} + b_{nM}F_{nM} + c_{nM}G_{nM} + d_{nM}H_{nM} + a_{nI}E_{nI} + b_{nI}F_{nI} + c_{nI}G_{nI} + d_{nI}H_{nI}) = -(\sigma_y^\infty - \sigma_x^\infty)\sin\theta_{i0}\cos\theta_{i0} \quad (22)$$

$$\sum_{n=1}^{M/2} (a_{nM}I_{nM} + b_{nM}J_{nM} + c_{nM}K_{nM} + d_{nM}L_{nM} + a_{nI}I_{nI} + b_{nI}J_{nI} + c_{nI}K_{nI} + d_{nI}L_{nI}) = -(\sigma_x^\infty - \nu_M\sigma_y^\infty)x/E_M$$

$$\sum_{n=1}^{M/2} (a_{nM}M_{nM} + b_{nM}N_{nM} + c_{nM}O_{nM} + d_{nM}P_{nM} + a_{nI}M_{nI} + b_{nI}N_{nI} + c_{nI}O_{nI} + d_{nI}P_{nI}) = -(\sigma_y^\infty - \nu_M\sigma_x^\infty)y/E_M$$

$$A_{nM} = (-1/2)t_n(\theta_i)\cos^2\theta_{i0}/\cos\theta_i + \int_0^{2\pi} K_{nnM}^{Fx}(\phi_k, \theta_i)t_n(\phi_k)bd\phi \quad (23)$$

$B_{nM}, \ldots, P_{nI}$ can be expressed in a similar manner.

The stresses at an arbitrary point are represented by a linear combination of the coefficients $a_{nM} \sim d_{nI}$, which is determined from the boundary conditions of suitably chosen collocation points shown in Eq. (24) and the influence coefficients corresponding to $A_{nM} \sim P_{nI}$.

Table 1 Convergence of the unknown functions ($a/b = 1$, $a/d = 0.648$, $\sigma_x^\infty = 1$, $\sigma_y^\infty = 0$, $E_I/E_M = 0.5$, $\nu_I = \nu_M = 0.3$, under plane stress in Fig. 1)

θ (deg.)	M	ρx3M	ρy2M	ρx1M	ρy4M
0	8	0.6938	0.0276	0.0282	-0.0420
	12	0.6938	0.0288	0.0283	-0.0440
	16	0.6938	0.0288	0.0283	-0.0440
20	8	0.7027	0.0205	0.0172	-0.0378
	12	0.7027	0.0208	0.0171	-0.0382
	16	0.7027	0.0208	0.0171	-0.0382
40	8	0.7186	0.0063	-0.0018	-0.0272
	12	0.7186	0.0061	-0.0016	-0.0269
	16	0.7186	0.0061	-0.0016	-0.0269
60	8	0.7291	-0.0042	-0.0127	-0.0182
	12	0.7292	-0.0040	-0.0128	-0.0186
	16	0.7292	-0.0040	-0.0128	-0.0186
80	8	0.7340	-0.0083	-0.0169	-0.0158
	12	0.7337	-0.0083	-0.0168	-0.0148
	16	0.7337	-0.0083	-0.0168	-0.0148
90	8	0.7348	-0.0087	-0.0174	-0.0157
	12	0.7342	-0.0088	-0.0172	-0.0144
	16	0.7342	-0.0088	-0.0172	-0.0144

θ (deg.)	M	ρx3I	ρy2I	ρx1I	ρy4I
0	8	1.4370	-0.0852	-0.3303	0.0898
	12	1.4377	-0.0853	-0.3313	0.0892
	16	1.4377	-0.0853	-0.3313	0.0892
20	8	1.3905	-0.0657	-0.2695	0.0738
	12	1.3899	-0.0653	-0.2686	0.0735
	16	1.3899	-0.0653	-0.2686	0.0735
40	8	1.3057	-0.0323	-0.1615	0.0464
	12	1.3061	-0.0326	-0.1622	0.0467
	16	1.3061	-0.0326	-0.1622	0.0467
60	8	1.2494	-0.0131	-0.0939	0.0295
	12	1.2491	-0.0129	-0.0935	0.0292
	16	1.2491	-0.0129	-0.0936	0.0292
80	8	1.2242	-0.0053	-0.0652	0.0214
	12	1.2244	-0.0053	-0.0653	0.0220
	16	1.2244	-0.0053	-0.0653	0.0220
90	8	1.2210	-0.0043	-0.0615	-0.0202
	12	1.2215	-0.0045	-0.0621	-0.0212
	16	1.2215	-0.0045	-0.0621	-0.0212

Table 2 Convergence of the stresses ($a/b = 1$, $a/d = 0.9$, $\tau_{xy}^\infty = 1$, $E_I = 0$ in Fig. 2)

θ (deg.)	M	σ_t	σ_n	τ_{nt}
40	16	-4.5587	-2.2×10^{-5}	-3.3×10^{-4}
	24	-4.5626	1.5×10^{-6}	1.9×10^{-6}
	32	-4.5627	6.9×10^{-6}	-9.1×10^{-6}
	40	-4.5627	2.2×10^{-7}	-5.7×10^{-6}
	48	-4.5627	4.9×10^{-7}	-1.7×10^{-7}
80	16	-2.7643	1.0×10^{-3}	2.7×10^{-3}
	24	-2.7675	3.9×10^{-5}	2.0×10^{-5}
	32	-2.7676	-1.0×10^{-6}	1.2×10^{-5}
	40	-2.7676	-2.9×10^{-6}	5.6×10^{-6}
	48	-2.7676	7.6×10^{-7}	-1.8×10^{-6}
90	16	-1.6283	-1.5×10^{-3}	-3.1×10^{-3}
	24	-1.6272	-9.6×10^{-5}	-3.2×10^{-5}
	32	-1.6272	-1.4×10^{-5}	1.9×10^{-5}
	40	-1.6272	-3.9×10^{-6}	8.9×10^{-6}
	48	-1.6272	-1.5×10^{-6}	4.2×10^{-6}
120	16	1.5923	-1.8×10^{-3}	1.7×10^{-3}
	24	1.5958	-1.7×10^{-4}	4.4×10^{-5}
	32	1.5959	8.6×10^{-6}	-2.3×10^{-5}
	40	1.5959	1.9×10^{-6}	-9.2×10^{-6}
	48	1.5959	-1.4×10^{-6}	8.3×10^{-6}
159.6	16	4.8794	-6.1×10^{-3}	3.7×10^{-4}
	24	4.8842	1.9×10^{-4}	-6.6×10^{-4}
	32	4.8863	-8.2×10^{-6}	1.3×10^{-5}
	40	4.8858	-2.9×10^{-7}	-1.3×10^{-5}
	48	4.8859	1.3×10^{-7}	-1.0×10^{-6}
160	16	4.8791	-5.6×10^{-3}	4.6×10^{-4}
	24	4.8828	1.5×10^{-4}	-5.3×10^{-4}
	32	4.8853	2.5×10^{-6}	-3.3×10^{-5}
	40	4.8847	-4.8×10^{-7}	-2.2×10^{-5}
	48	4.8848	3.5×10^{-7}	-2.9×10^{-6}

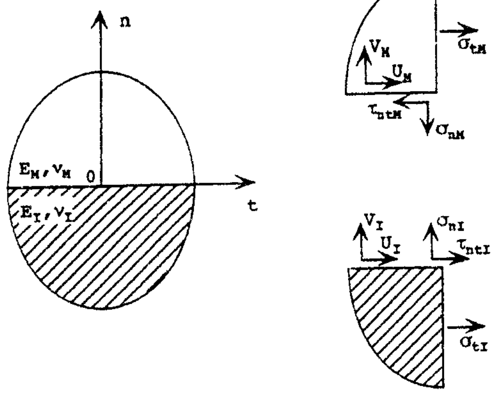

Fig. 4 Model of interface

Table 5 Values and positions of the maximum stress for two circular inclusions ($a/b = 1$, $\sigma_x^\infty = 1$, $\sigma_y^\infty = 0$, $\nu_I = \nu_M = 0.3$, plane strain in Fig. 1)

		Matrix		Inclusion	
EI/EM	a/d	(deg.)	σmax	(deg.)	σmax
0.0	0.	90.0	3.0000		
	0.1	90.0	2.9804		
	0.2	89.7	2.9268		
	0.3	89.0	2.8531		
	0.4	88.0	2.7774		
	0.5	86.7	2.7065		
	0.6	85.9	2.6704		
	0.7	85.2	2.6419		
	0.8	84.7	2.6234		
	0.9	84.4	2.6114		
0.5	0.	90.0	1.5058	0~180	0.7573
	0.1	90.0	1.5034	0.	0.7562
	0.2	89.9	1.4966	0.	0.7533
	0.3	89.7	1.4868	0.	0.7492
	0.4	89.4	1.4759	0.	0.7442
	0.5	89.0	1.4659	33.5	0.7388
	0.6	88.6	1.4581	60.5	0.7338
	0.7	88.4	1.4532	76.0	0.7298
	0.8	88.2	1.4509	86.8	0.7274
	0.9	88.1	1.4510	94.3	0.7265
2.0	0	22.4,157.6	1.2149	0~180	1.1920
	0.1	157.6	1.2166	180.	1.1937
	0.2	157.8	1.2225	180.	1.1997
	0.3	158.0	1.2338	180.	1.2115
	0.4	158.8	1.2516	180.	1.2310
	0.5	160.7	1.2774	180.	1.2607
	0.6	163.6	1.3134	180.	1.3034
	0.7	169.3	1.3642	180.	1.3618
	0.8	180.0	1.4370	180.	1.4370
	0.9	180.0	1.5192	180.	1.5192
∞	0.	21.7158.3	1.5488	0~180	1.4778
	0.1	158.2	1.5546	180.	1.4833
	0.2	158.2	1.5747	180.	1.5025
	0.3	158.3	1.6135	180.	1.5433
	0.4	159.7	1.6776	180.	1.6131
	0.5	162.7	1.7777	180.	1.7263
	0.6	166.2	1.9348	180.	1.9055
	0.7	180.0	2.1932	180.	2.1932
	0.8	180.0	2.6900	180.	2.6933
	0.9	160.0	3.7657	180.	3.4197

Table 6 Values and positions of the maximum stress for two circular inclusions ($a/b = 1$, $\sigma_x^\infty = 0$, $\sigma_y^\infty = 1$, $\nu_I = \nu_M = 0.3$, plane strain in Fig. 1)

		Matrix		Inclusion	
EI/EM	a/d	(deg.)	σmax	(deg.)	σmax
0.0	0	0.,180.	3.0000		
	0.1	0.	3.0005		
	0.2	0.	3.0043		
	0.3	0.	3.0147		
	0.4	0.	3.0345		
	0.5	0.	3.0642		
	0.6	180.	3.1162		
	0.7	180.	3.3807		
	0.8	180.	4.0340		
	0.9	180.	5.7993		
0.5	0.	0.,180.	1.5058	0.~180.	0.7573
	0.1	0.	1.5060	124.5	0.7576
	0.2	0.	1.5065	124.5	0.7584
	0.3	0.	1.5076	126.8	0.7602
	0.4	180.	1.5096	132.5	0.7635
	0.5	180.	1.5159	141.5	0.7694
	0.6	180.	1.5313	157.0	0.7796
	0.7	180.	1.5676	180.	0.8006
	0.8	180.	1.6495	180.	0.8436
	0.9	180.	1.8375	180.	0.9360
2.0	0	67.7,112.3	1.2149	0.~180.	1.1920
	0.1	67.6	1.2147	0.	1.1918
	0.2	67.6	1.2142	0.	1.1914
	0.3	67.6	1.2162	0.	1.1909
	0.4	67.5	1.2116	0.	1.1904
	0.5	67.4	1.2091	0.	1.1901
	0.6	67.2	1.2059	0.	1.1899
	0.7	67.0	1.2020	0.	1.1901
	0.8	66.7	1.1976	0.	1.1905
	0.9	66.4	1.1931	0.	1.1913
∞	0	68.3,111.7	1.5488	0.~180.	1.4778
	0.1	68.2	1.5488	0.	1.4775
	0.2	68.2	1.5490	0.	1.4778
	0.3	68.3	1.5491	0.	1.4800
	0.4	68.3	1.5487	0.	1.4852
	0.5	68.4	1.5479	0.	1.4945
	0.6	68.5	1.5467	0.	1.5093
	0.7	68.6	1.5456	0.	1.5308
	0.8	68.7	1.5455	0.	1.5612
	0.9	68.9	1.5474	0.	1.6098

First, to examine the accuracy of the present analysis, subtraction of interface stresses and displacements $(\sigma_{nM} - \sigma_{nI})$, $(\tau_{ntM} - \tau_{ntI})$, $(\epsilon_{tM} - \epsilon_{tI})$, $(U_M - U_I)$, $(V_M - V_I)$ are calculated for the problem when $a/b = 1$, $a/d = 0.648$, $\sigma_x^\infty = 1$, $\sigma_y^\infty = 0$, $E_I/E_M = 0.5$, $\nu_I = \nu_M = 0.3$, under plane stress in Fig. 1. These values, that should be zero along the interface, are less than 10^{-5} even when $M = 12$. Table 3 shows interface stresses and values of Eq. (29). Table 4 shows interface strains and values of Eq. (31) and Eq. (32). It is found that the present method satisfy these conditions to the sixth digit. In the present analysis, therefore, the boundary requirements can be highly satisfied along the entire boundary.

7 Interaction Between Two Elliptical Holes Under Tension

Tables 5 and 6 show values and positions of maximum stress (principal stress) under plane strain for two circular inclusions. From the results of Tables 5 and 6, it is found that the values and positions of the maximum stress slightly varies with varying the shape and elastic ratio. The interaction effect is not very large unless the inclusions are extremely close ($a/d \geqq 0.8$) and elastic ratio between matrix and inclusion are extremely different ($E_I/E_M = 0$ or $E_I/E_M = \infty$). The calculations are carried out also for plane stress. The results of Shioya (1971) are in good agreement with the present results when $a/d = 0.465$, 0.648, and $E_I/E_M = 0.5$, 2.0.

Figures 5–8 show the stress distribution $(\sigma_1, \sigma_n, \sigma_t, \tau_{nt})$ along the boundary of matrix when $E_I/E_M = 0.0, 0.5, 2.0, \infty$ under $\sigma_x^\infty = 1$, $\sigma_y^\infty = 0$. The solid line shows the stress distribution when $a/d = 0.9$ ($E_I/E_M = 0.0, 0.5, 2.0$) or $a/d = 0.5$ ($E_I/E_M = \infty$) and the broken line shows the stress distribution when $a/d \to 0$. The present method is useful for obtaining these smooth stress distributions.

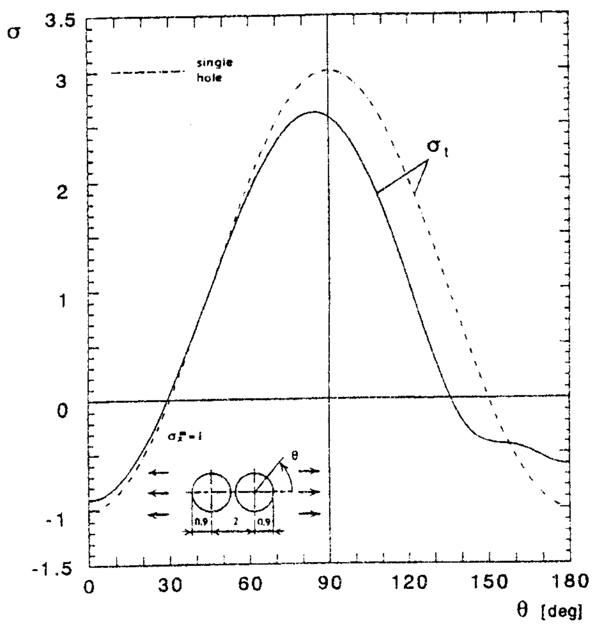

Fig. 5 Stress distribution of hole ($\sigma_x^\infty = 1$, $\sigma_y^\infty = 0$ in Fig. 1)

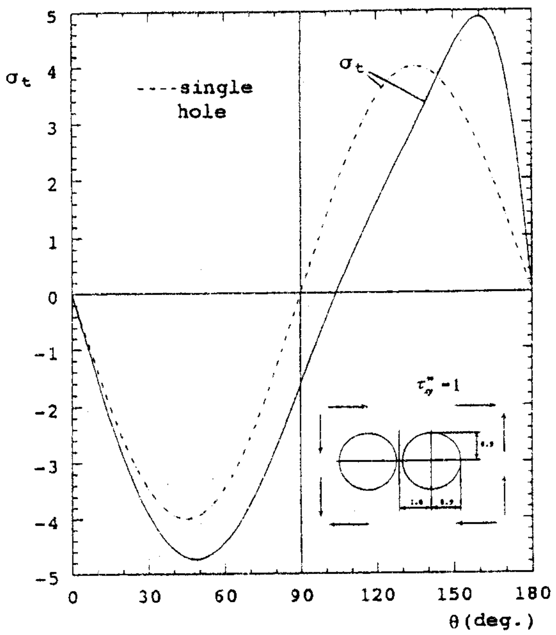

Fig. 9 Stress distribution of hole (τ_{xy}^{∞} = 1, E_I = 0 in Fig. 2)

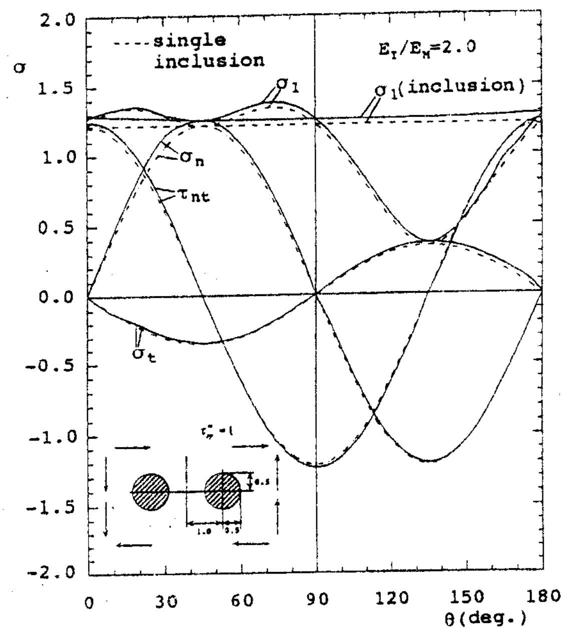

Fig. 11 Stress distribution of matrix (τ_{xy}^{∞} = 1, E_I = E_M = 2.0, ν_I = ν_M = 0.3, plane strain in Fig. 2)

1 The interaction problem between elliptical inclusion was formulated in terms of singular integral equations with Cauchy-type and logarithmic-type singularities. To formulate the problem, the body force method was applied, where the stress and displacement fields due to a point force were used as the fundamental solutions. The problem is reduced to determining the unknown body force densities distributed in infinite plates having the same elastic constants as those of the matrix and inclusions.

2 To determine the unknown body-force densities to satisfy the boundary conditions, four auxiliary unknown functions were defined from each body-force density. It is found that determining four auxiliary functions in the range $0 \leqq \phi_k \leqq \pi/2$ is equivalent to determining a original unknown density in the range $0 \leqq \phi_k \leqq 2\pi$. Namely, if the auxiliary functions are given in the range $0 \leqq \phi_k \leqq \pi/2$, the original unknown function is expressed in the range $0 \leqq \phi_k \leqq 2\pi$. Then, instead of determining body-force densities directly, these auxiliary unknowns were approximated by using known fundamental densities and unknown weight functions. Here, the fundamental density was defined as an example of continuous function holding the condition that the auxiliary function must satisfy. The solution presented in this paper will be applied to several problems in the following paper and the results and usefulness will be discussed.

3 Two elliptical inclusions under remote tension were considered. The accuracy of the present analysis was verified

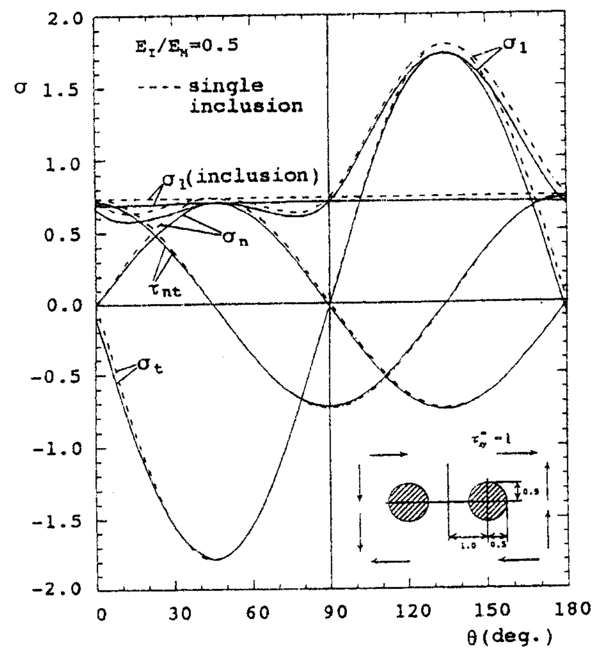

Fig. 10 Stress distribution of matrix (τ_{xy}^{∞} = 1, E_I = E_M = 0.5, ν_I = ν_M = 0.3, plane strain in Fig. 2)

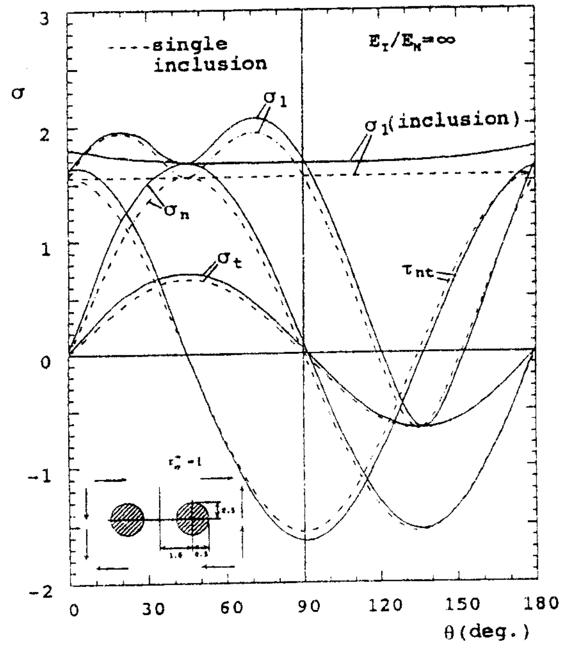

Fig. 12 Stress distribution of matrix (τ_{xy}^{∞} = 1, E_I = E_M = ∞, ν_I = ν_M = 0.3, plane strain in Fig. 2)

through examining the convergence of the results and necessary relations between interface stresses, strains, and displacements. The maximum stresses and stress distributions along the interface were shown in the tables and charts.

4 Two elliptical inclusions under remote shear were also considered. The results were shown in the tables and charts. With increasing a/d, the maximum stress for two circular holes has a peak value at a midpoint of a/d and it decreases as $a/d \to 1$.

5 The usefulness of the theory and solutions in the preceding paper was confirmed for the wide geometrical and elastic ranges of inclusions. The method may be applied to regular or random distributions of inclusions.

References

Barrett, R. F., Sheth, P. R., and Patel, G. C., 1971, "Effect of Two Circular Holes in a Plate Subjected to Pure Shear Stress," ASME JOURNAL OF APPLIED MECHANICS, Vol. 93, pp. 528–530.

Donnel, L. H., 1974, *Stress Concentration Factors*, R. E. Peterson, ed., John Wiley and Sons, New York, p. 223.

Erdogan, F., and Gupta, G. D., 1972, "On the Numerical Solution of Singular Integral Equations," *Quarterly Applied Mathematics*, Vol. 30, pp. 525–534.

Eshelby, J. D., 1957, "The Determination of the Elastic Field of an Ellipsoidal Inclusion, and Related Problems," *Proceedings Royal Society of London.*, Vol. A241, pp. 376–396.

Eshelby, J. D., 1959, "The Elastic Field Outside an Ellipsoidal Inclusion," *Proceedings Royal Society of London.*, Vol. A252, pp. 561–569.

Mura, T., 1987, *Micromechanics of Defects in Solids*, 2nd Ed., Martinus Nijhoff, Boston, MA, pp. 129–176.

Mura, T., 1988, "Inclusion Problems," ASME *Applied Mechanics Reviews*, Vol. 41, pp. 129–176.

Nisitani, H., 1963, "On the Tension of an Infinite Plate Containing an Infinite Row of Elliptical Holes," *Bull. Japan Soc. Mech. Eng.*, Vol. 6, pp. 635–638.

Nisitani, H., 1967, "The Two-Dimensional Stress Problem solved using an Electrical Digital Computer," *Jour. Japan Soc. Mech. Eng.*, Vol. 70, pp. 627–632. (*Bull. Japan Soc. Mech. Eng.*, Vol. 11, 1968, pp. 14–23).

Nisitani, H., 1968, "Method of Approximate Calculation for Interference Effects and Its Application," *J. Japan Soc. Mech. Eng.*, Vol. 11, pp. 725–738.

Nisitani, H., 1974, "Solution of Notch Problems by Body Force Method," *Stress Analysis of Notch Problem* G. C. Sih, ed., Leyden, pp. 1–68.

Nisitani, H., and Chen, D. H., 1987, *Taisekiryokuhou*, Baifukan, p. 89 (in Japanese).

Noda, N.-A., and Matsuo, T., 1995a, "Singular Integral Equation Method in the Analysis of Interaction between Crack and Defects," *Fracture Mechanics* ASTM STP 1220, F. Erdogan, ed., American Society for Testing and Materials, Philadelphia, pp. 591–605.

Noda, N.-A., and Matsuo, T., 1995b, "Singular Integral Equation Method in Optimization of Stress-Relieving Hole: A New Approach Based on the Body Force Method," *Int. Jour. Fract.*, Vol. 70, pp. 147–165.

Noda, N.-A., and Matsuo, T., 1997, "Numerical Solution of Singular Integral Equations in Stress Concentration Problems," *International Journal Solids Structures*, Vol. 34, No. 19, pp. 2429–2444.

Shioya, S., 1971, "On the Tension of an Infinite Thin Plate Containing a Pair of Circular Inclusions," *Bulletin of the JSME*, Vol. 14, No. 68, pp. 117–126.

APPENDIX

Fundamental Solutions

The kernel of stresses and displacement used in Eqs. (1), (2) are expressed by putting $F_x = 1$, $F_y = 1$ in Eq. (A1)–(A3).

(a) Stress:

$$K_{nn}^{Fx} = \sigma_n^{Fx} = \sigma_x^{Fx}\cos^2\theta + \sigma_y^{Fx}\sin^2\theta + 2\tau_{xy}^{Fx}\sin\theta\cos\theta$$

$$K_{nn}^{Fy} = \sigma_n^{Fy} = \sigma_x^{Fy}\cos^2\theta + \sigma_y^{Fy}\sin^2\theta + 2\tau_{xy}^{Fy}\sin\theta\cos\theta$$

$$K_{nt}^{Fx} = \tau_{nt}^{Fx} = (-\sigma_x^{Fx} + \sigma_y^{Fx})\sin\theta\cos\theta + 2\tau_{xy}^{Fx}(\cos^2\theta - \sin^2\theta)$$

$$K_{nt}^{Fy} = \tau_{nt}^{Fy} = (-\sigma_x^{Fy} + \sigma_y^{Fy})\sin\theta\cos\theta + 2\tau_{xy}^{Fy}(\cos^2\theta - \sin^2\theta) \quad \text{(A1)}$$

where

$$\sigma_x^{Fx} = -\frac{(x-\xi)\{\beta(x-\xi)^2 + \alpha(y-\eta)^2\}}{r^4}F_x$$

$$\sigma_x^{Fy} = \frac{(y-\eta)\{\alpha(y-\eta)^2 + (2\alpha-\beta)(x-\xi)^2\}}{r^4}F_y$$

$$\sigma_y^{Fx} = \frac{(x-\xi)\{\alpha(x-\xi)^2 + (2\alpha-\beta)(y-\eta)^2\}}{r^4}F_x$$

$$\sigma_y^{Fy} = \frac{(y-\eta)\{\beta(y-\eta)^2 + \alpha(x-\xi)^2\}}{r^4}F_y$$

$$\tau_{xy}^{Fx} = -\frac{(y-\eta)\{\beta(x-\xi)^2 + \alpha(y-\eta)^2\}}{r^4}F_x$$

$$\tau_{xy}^{Fy} = -\frac{(x-\xi)\{\beta(y-\eta)^2 + \alpha(x-\xi)^2\}}{r^4}F_y$$

$$r^2 = (x-\xi)^2 + (y-\eta)^2,$$

$$\alpha = \frac{1-\nu}{4\pi}, \quad \beta = \frac{3+\nu}{4\pi} \quad \text{(plane stress).} \quad \text{(A2)}$$

(b) Displacement:

$$K_u^{Fx} = \left[2\gamma\log\frac{R}{r} + \delta\left\{\frac{(x-\xi)^2-(y-\eta)^2}{r^2} - \frac{\xi^2-\eta^2}{R^2}\right\}\right]F_x$$

$$K_u^{Fx} = 2\delta\left[\frac{(x-\xi)(y-\eta)}{r^2} - \frac{\xi\eta}{R^2}\right]F_y$$

$$K_V^{Fx} = 2\delta\left[\frac{(x-\xi)(y-\eta)}{r^2} - \frac{\xi\eta}{R^2}\right]F_x$$

$$K_V^{Fy} = \left[2\gamma\log\frac{R}{r} + \delta\left\{\frac{(x-\xi)^2-(y-\eta)^2}{r^2} - \frac{\xi^2-\eta^2}{R^2}\right\}\right]F_y$$

$$\gamma = \frac{(1+\nu)(3-\nu)}{8\pi E}, \quad \delta = \frac{(1+\nu)^2}{8\pi E},$$

$$R^2 = \xi^2 + \eta^2 \quad \text{(plane stress).} \quad \text{(A3)}$$